2020 IEEE International Conference on Robotics and Automation (ICRA)
31 May - 31 August, 2020. Paris, France

Novel Proximity Sensor for Realizing Tactile Sense in Suction Cups

Sayaka Doi[1], Hiroki Koga[1], Tomonori Seki[1] and Yutaro Okuno[1]

***Abstract*— We propose a new capacitive proximity sensor that detects deformations of a suction cup as a tactile sense. We confirmed that one sensor module provides three applications for reliable picking and a simplified setup. The first application is the picking height decision. The second one is the placing height decision for detecting whether the grasped object is placed on the placement surface. These two applications are achieved by detecting the push-in stroke of the suction cup. The final application is detection of whether the suction cup is in partial contact or full contact with the object. This function can correct the picking posture as well as detect whether picking is possible before the pull-up motion. We also demonstrate that the partial contact position can be estimated in real time.**

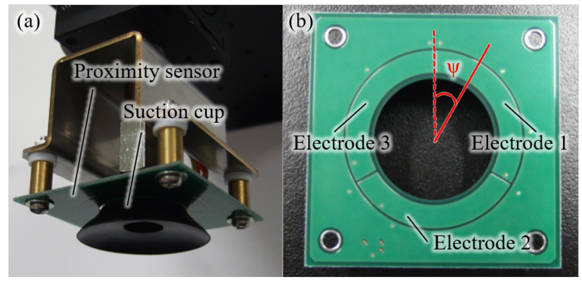

Fig. 1. Prototype sensor. (a) Suction cup with proximity sensor. (b) Electrodes of capacitive proximity sensor.

I. INTRODUCTION

Industrial robots (e.g., articulated robots, selective compliance articulated robot arms (SCARA robots), and parallel robots) are widely used in factores. However, to meet task-yield and cycle-time requirements, skillful engineers need to teach robots the correct positions and/or design dedicated jigs. They often need to verify the teaching positions and cycle times repeatedly. These setup methods tend to be expensive and take a long time. Mass production has used automated systems with industrial robots, but small and medium-sized production have had problems incorporating industrial robots because automation costs may outweigh their effect. Despite this, the demand for automation of small or medium-sized production is growing due to declines in the labor force and rising wages.

Numerous techniques using visual systems have been proposed for pick-and-place operations [1], [2]. While these are effective in various situations in factories, visual sensors typically have difficulty recognizing objects depending on their material, texture, and color. They also have occlusion and lighting disturbance problems. For these reasons, it has been proposed to use vision sensors in combination with other sensors.

Tactile and/or proximity sensors mounted on the fingers of a robot end-effector have been proposed for reliable picking. Techniques that use tactile sensors to detect the grasping force or contact geometry [3]–[5] have demonstrated stable grasping. Moreover, proximity sensors have been proposed as intermediates between tactile and vision sensors [6]–[10]. Picking can be reliably performed by detecting the distance between the finger and the object. Techniques combining proximity and tactile sensors have also been proposed [3], [11]–[14]. A number of studies have shown that tactile or proximity sensors mounted on the robot's end-effector are useful for manipulation.

While various sensors have been proposed for multi-fingered end-effector applications, there are few proposals of sensors for vacuum suction-cup applications. Manipulation systems using suction cups are common, in part because it is easy to plan and control suction cups for grasping [15], [16]. In the 2017 Amazon Robotics Challenge and the 2018 World Robot Challenge, many teams used suction-cup manipulation systems. Since the suction cup has a soft rubber part, position errors can be absorbed by the rubber stroke. Nevertheless, picking failures, which are presumed to be mainly due to recognition errors by the visual sensor system, often occurred in these challenges, and the grasped object was released before it touched the placement surface. In an actual application, this problem would pose a risk of dropping or breakage of the object. Moreover, precise placement is difficult in an actual application. These issues lead to poor task yield and poor product quality. Thus, suction cups besides other end-effectors are required for teaching precise positions, and a dedicated jig is needed to eliminate position errors.

Pressure and flow sensors are often used to detect picking failures after a pick-up procedure with a suction cup, e.g. [17]. A force-torque sensor attached to the wrist of the robot was used for detecting contact with objects in [17], [18]. Although the results showed their effectiveness, force-torque sensors are expensive. In addition, there is concern about low sensitivity when the sensor is attached to the base of a soft end-effector such as a suction cups, because the effector works as a damper. An array of flexible piezoresistive tactile sensors was proposed for vacuum suction cups and magnetic grippers [19]. This technique has the advantage that the sensor, which is attached to the gripping surface, can be applied to magnetic grippers as well as suction cups. However, damage may occur to the sensor or object when

[1]Sayaka Doi, Hiroki Koga, Tomonori Seki and Yutaro Okuno are with OMRON Corporation, Kizugawadai 9-1. Kizugawa-city, Kyoto, Japan { sayaka.doi, hiroki.koga, tomonori.seki, yutaro.okuno }@omron.com

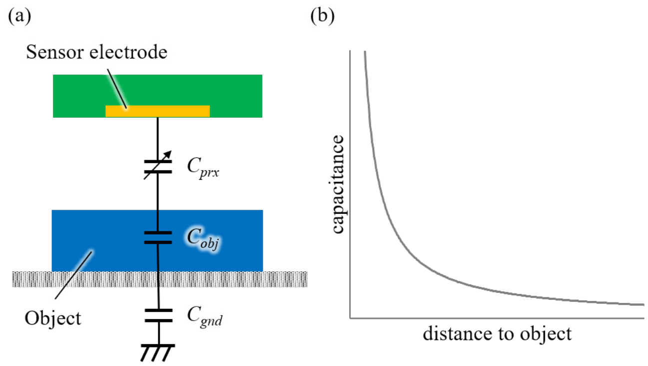

Fig. 2. Typical capacitive proximity sensor. (a) Scheme of main capacitance formed by sensor electrode. (b) Relationship between measured capacitance and distance from sensor electrode to object.

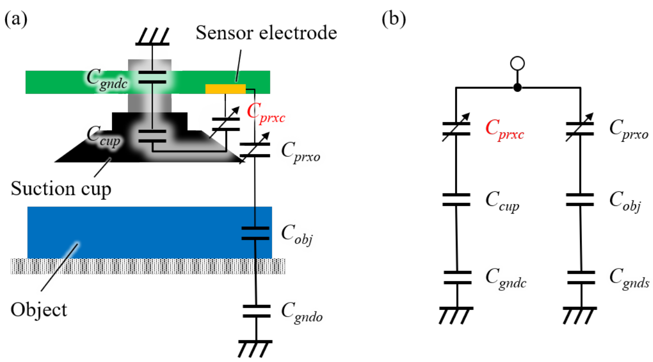

Fig. 3. Proposed sensor. (a) Scheme of main capacitance formed by sensor electrode. (b) Equivalent circuit of the sensor.

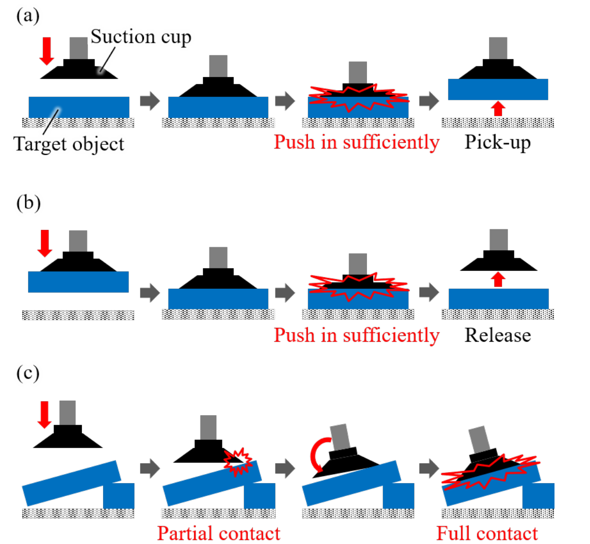

Fig. 4. Applications of the sensor. (a) Picking control by detecting push-in. (b) Placing control by detecting push-in. (c) Posture control by detecting partial contact.

they are in contact.

Under these circumstances, we decided to develop a sensor for suction cups (Fig. 1). Specifically, the purpose of our study was to make setup of automation easy with a reasonable sensor. The purpose of this our study is to make setup of automation easy with practical sensor. The proposed sensor gives a tactile sense to the suction cup, and it is both simple and low-cost. The sensor has the potential to make a manipulation system without the need for teaching the robot the precise positions or for building a dedicated jig.

II. SENSOR DEVELOPMENT

A. Capacitive Proximity Sensing

This section describes the principle of operation of the capacitive proximity sensor. Figure 2(a) shows the schematic diagram of the capacitance formed by the electrode of a typical capacitive proximity sensor. In accordance with the parallel plate capacitance model, the capacitance is proportional to the permittivity and electrode size, and it is inversely proportional to the distance to object, as shown in Fig. 2(b). C_{prx} is the capacitance between the electrode and the object, and it depends on the distance between them. C_{obj} indicates the capacitance of the object itself, which depends on its permittivity and shape. When the object is a conductor such as a metal, C_{obj} can be ignored (short circuit). In the case of a dielectric object made from, e.g., plastic, the measured capacitance is affected by C_{obj}. C_{gnd} indicates the grounding state of the object. When the object is directly grounded, C_{gnd} can be ignored (short circuit). When the object is not explicitly grounded, the measured capacitance is most affected by C_{gnd}. The measured capacitance is the total capacitance of C_{prx}, C_{obj}, and C_{gnd} in series. When C_{obj} and C_{gnd} can be ignored, the measured capacitance is large and the measurement has high sensitivity. When C_{obj} and C_{gnd} are small, the measured capacitance is small and the measurement has low sensitivity.

B. Sensor Design

Photographs of the prototype capacitive proximity sensor are shown in Fig. 1. Three electrodes are arranged on one side of the sensor board (Fig. 1(b)). These electrodes can determine partial contact without having to use too small an electrode. The outer diameters of the electrodes are 35 mm, which is the same as that of the suction cup. In the center of the sensor, a cutout hole is prepared for the suction cup. To measure capacitance, we used a self-capacitive digital converter FDC1004 made by Texas Instruments. It is mounted on the other side of the sensor board. The sample rate of the FDC1004 is 100 Hz, using a microcontroller (Arduino Uno). The sensor is attached to the suction cup (Fig. 1(a)).

Figure 3 shows the scheme of the capacitances of the sensor and the equivalent circuit. Although there would be a capacitance between the suction cup and the object, it is omitted here for the sake of simplicity. Compared with Fig. fig2(a), a route via the suction cup is added. C_{prxc} is the capacitance between the electrode and the suction cup, and C_{prxo} is the capacitance between the electrode and the object. These capacitances correspond to C_{prx} in Fig. 2(a).

C_{cup} and C_{obj} are the capacitance of the suction cup and that of the object, respectively, while C_{gndc} and C_{gndo} are the grounded state capacitance of the suction cup and that of the object, respectively. The measured capacitance is the sum of the series capacitances of the suction cup route (C_{prxc}, C_{cup} and C_{gndc}) and that of the object route (C_{prxo}, C_{obj} and C_{gndo}).

C. Applications

Figure 4 shows three possible applications of the sensor in pick-and-place operations. In picking operations (Fig. 4(a)), the sensor detects whether a push-in stroke is sufficient to grasp an object, and the robot can decide the picking height by itself without being taught. This application is also compatible with non-uniform objects, for which it is difficult to set the picking height in advance. In placing operations (Fig. 4(b)), the sensor detects whether the grasped object is placed on the surface without the robot having been taught the placing height. Both the height of the surface and the height of the object are usually needed in advance for careful placement, but this determination becomes unnecessary in our system. Figure 4(c) shows a picking operation in the case of a tilted object. Partial contact between the suction cup and the object leads to a picking failure due to air leaking into the suction cup after negative pressure has been applied. The robot can correct the posture of the suction cup from the information on the partial contact position detected by the sensor.

III. CAPACITIVE TACTILE SENSING

Here, we describe the estimation methods of the push-in stroke l and the partial contact position ψ. l is the displacement of the lip position before and after deformation. ψ is the clockwise rotation angle, as shown in Fig. 1(b).

We used the following linear regression to estimate the push-in stroke l:

$$l = \alpha \Delta C + \beta, \tag{1}$$

where the coefficient α and β are experimentally obtained from 10 measurements. Three times the standard deviation (3σ) is 6.3 fF for three measurements, and it is equivalent to a fluctuation in l of about 0.14 mm. On the other hand, 3σ is 4.5 fF at 10 measurements, and it is equivalent to a fluctuation in l of about 0.09 mm. This is sufficient to detect the push-in stroke in practice. ΔC is the sum of the measured capacitive displacements obtained from the three electrodes as follows:

$$\Delta C = \Delta C_1 + \Delta C_2 + \Delta C_3, \tag{2}$$

where the subscripts are the electrode's number.

To estimate the partial contact position ψ, the capacitive displacements obtained from the three electrodes are approximated as follows:

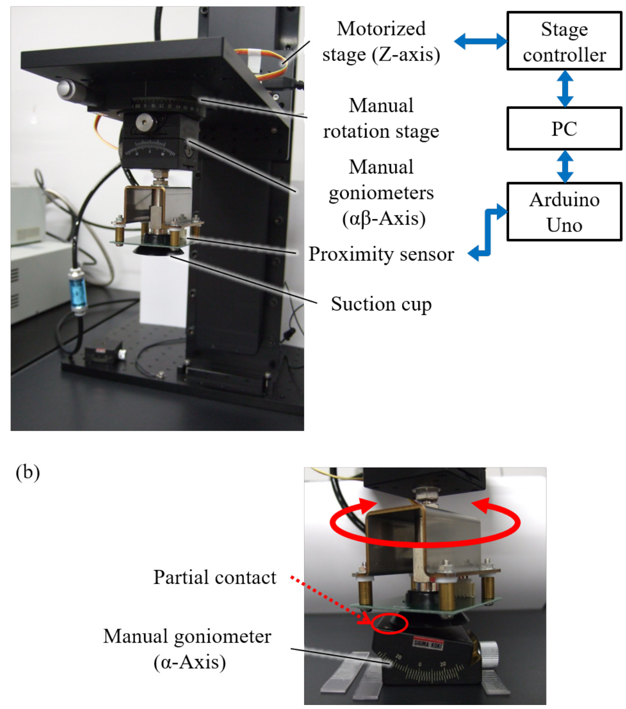

Fig. 5. Experimental setup. (a) Common setup for the experiments. (b) Setup for the partial contact experiments.

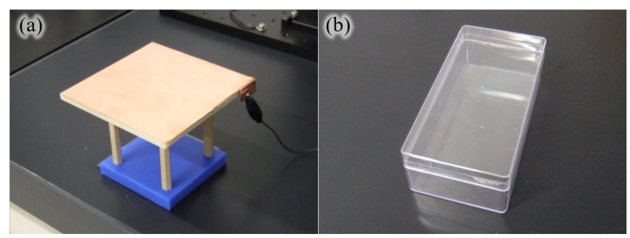

Fig. 6. Sample objects used in the experiments. (a) Grounded copper sheet. (b) Plastic case.

$$\Delta C_1 = A\cos(\psi - 60^\circ) + B, \tag{3}$$
$$\Delta C_2 = A\cos(\psi + 180^\circ) + B, \tag{4}$$
$$\Delta C_3 = A\cos(\psi + 60^\circ) + B, \tag{5}$$

where A and B are coefficients, but they do not need to be derived in order to find ψ. We can get the following equation by solving the system of equations (3), (4), and (5):

$$\psi = \tan^{-1} \frac{\sqrt{3}(\Delta C_1 - \Delta C_3)}{\Delta C_1 + \Delta C_3 - 2\Delta C_2}. \tag{6}$$

We judge that the state is in full contact when each electrode's ΔC is larger than a certain value.

IV. EXPERIMENTS AND DISCUSSION

A. Experimental Setup

The common setup used for the experiments is shown in Fig. 5(a). To evaluate push-in stroke, we used a motorized Z-

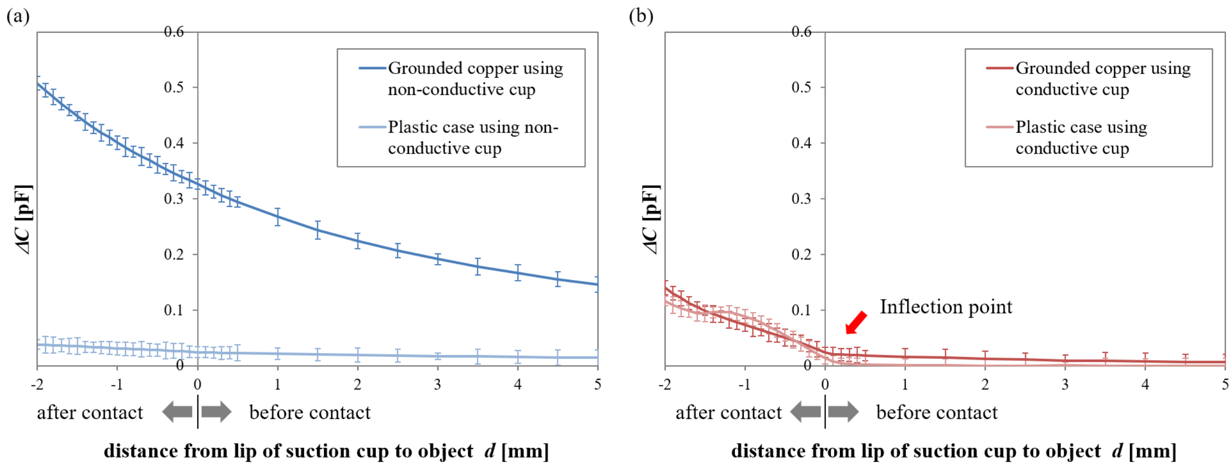

Fig. 7. Capacitive displacement data of push-in stroke experiments using non-conductive cup (a) and using conductive cup (b). The data are the means $\pm 3\sigma$ (n $=$ 10) for d from -2 to 5 mm.

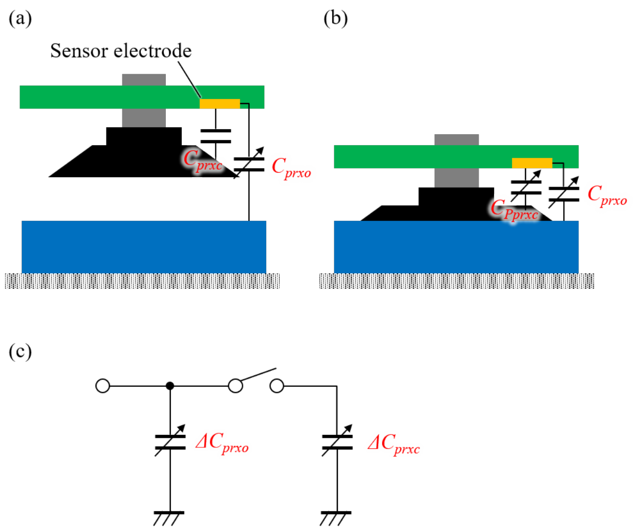

Fig. 8. Capacitance before contact (a) and after contact (b). (c) Equivalent circuit of ΔC when the suction cup is conductive.

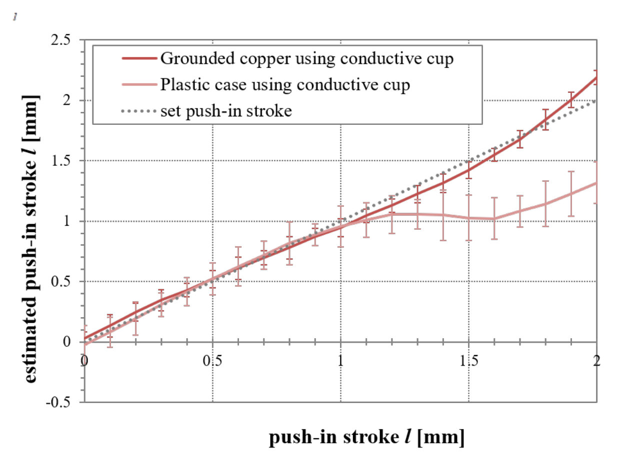

Fig. 9. Estimation results of push-in stroke when the push-in stroke l is 0 to 2 mm. The estimation data are the means $\pm 3\sigma$ (n $=$ 10).

axis stage (OSMS26-300 from Sigmakoki). The suction cup with the sensor was attached to the Z-axis stage via manual $\alpha\beta$-axis goniometers and a rotation stage (KSP-606M, GOH-40B15 from Sigmakoki). A stage controller was used to control the stage and observe its position. To evaluate partial contact, we used a manual α-axis goniometer as an object, as shown in Fig. 5(b). We set the tile angle of partial contact to 10° by using the α-axis goniometer after adjusting the tilt to be in the full contact state by the $\alpha\beta$-axis goniometers at 0° of the α-axis goniometer.

We evaluated the push-in stroke using suction cups made of two rubber materials: non-conductive silicone and conductive silicone (PFG-35-S/PFG-35-SE from Myotoku). The conductive cup was grounded. As shown in Fig. 6, we tested two objects: a grounded copper sheet and plastic case. These objects have rather different sensitivities, as described in II-A, which cover the range of most objects.

B. Results of Push-in Experiments

The results of the push-in stroke experiments using the non-conductive and conductive cups are shown in Fig. 7(a) and Fig. 7(b), respectively. The vertical axes express ΔC, and the horizontal axes express the distance d between the lip of the suction cup and the object. $d = 0$ mm when the cup just touches the object, $d > 0$ mm is the state before contact, and $d < 0$ mm is the state after contact. In Fig. 7, the capacitive displacement data are the means of 10 measurements, and the error bars indicate 3σ. As shown in Fig. 7(a), when the suction cup is non-conductive, ΔC is inversely proportional to d, and this relationship is like that of a typical capacitive proximity sensor as in Fig. 2(b). While the sensitivity of the grounded copper is high, the sensitivity of the plastic case is very low. On the other hand, when the suction cup is conductive, the results for the grounded copper line and plastic line mostly overlap, and each line has an inflection point near $d = 0$ mm, as shown in Fig. 7(b). The overlap means that the sensitivity of the plastic

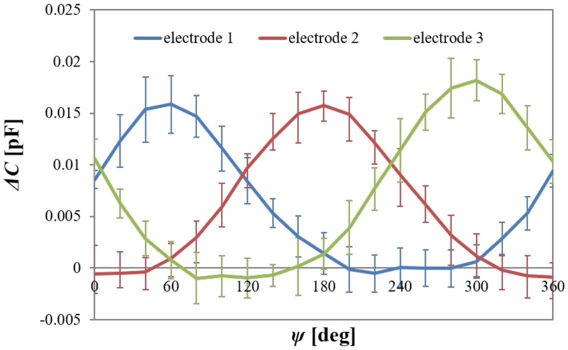

Fig. 10. Measurements gathered in partial contact experiments using conductive silicone cup. The data are the means $\pm 3\sigma$ (n = 10).

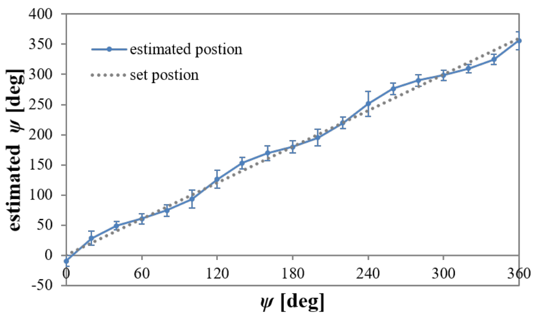

Fig. 11. Estimated partial contact position ψ. The estimated data are the means $\pm 3\sigma$ (n = 10).

case is similar to that of grounded copper, and adjustment of the sensitivity for each object is unnecessary. Compared with the non-conductive cup, the sensitivity of the conductive cup after contact with the plastic case is high.

Figure 8 shows images of the capacitance and equivalent circuit of the capacitance measured when using the conductive cup. C_{cup}, C_{gndc}, C_{obj} and C_{gndo} in Fig, 3 are omitted. When using the grounded conductive cup, C_{cup} and C_{gndc} in Fig. 3(b) are almost ignorable (short circuit) and the measured ΔC is approximately equal to ΔC_{prxc} because C_{prxc} is much larger than C_{prxo} ($C_{prxc} \gg C_{prxo}$). Consequently, while ΔC is hardly detected before contact because C_{prxc} does not change (Fig. 8(a)), it has a large value after contact (Fig. 8(b)). This behavior is like that of a switch circuit (Fig. 8(c)). Turning on the switch means contact with the object. An inflection point appears due to this switch mechanism. In theory, ΔC_{prxo} becomes large after contact, becase the distance to the object is small. The overlapping results confirmed that the relationship of $C_{prxc} \gg C_{prxo}$ is strong. The benefits of using the conductive cup can be briefly summarized as follows:

- Easy to detect contact from the inflection point
- Possible to detect any object
- No need to adjust the sensitivity

Therefore, we decided to use only the conductive cup in the subsequent evaluations.

Figure 9 shows the estimated push-in stroke l. l is equivalent to $-d$ at $d < 0$ mm. The coefficients α and β in (1) were calculated from the measured data of the grounded copper sheet, and they were used to estimate l with the plastic case as well as the grounded copper sheet. When l was from 0 to 1 mm, good estimations of push-in stroke were achieved for both objects. Although good estimation results were obtained for the copper sheet when l was from 1 to 2 mm, the estimated strokes were shifted for the plastic case. This is due to the fact that the effect of ΔC_{prxo} is larger as the distance to the object gets smaller. In pick-and-place applications that use thresholds of the push-in stroke, this shift at $l > 1$ mm is not a significant issue, as the accuracy immediately after contact is more important.

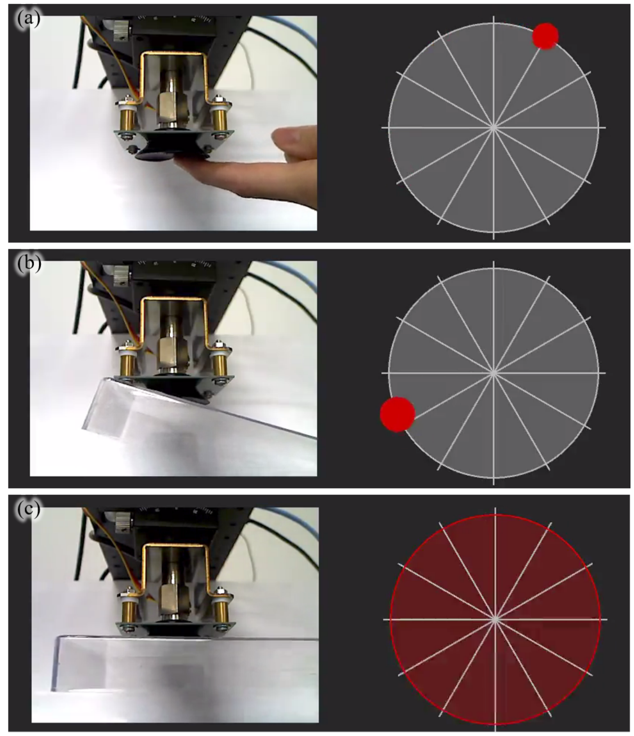

Fig. 12. Real-time estimation examples of partial contact position when object is a finger (a) and plastic case (b). Full-contact estimation example with plastic case (c).

C. Results of Partial Contact Experiments

The results of the partial contact experiments are shown in Fig. 10. The vertical axis expresses ΔC and the horizontal axis expresses the contact position ψ. The data are the means $\pm 3\sigma$ (n = 10). The peak of the three capacitive displacements changes every 120°. This is consistent with the relationship between ψ and the positions of the electrodes. Figure 11 shows ψ estimated from the measurement data in Fig. 10. At about 0°, 120°, and 240°, the error range is larger than elsewhere. These positions are discontinuous portions of the electrodes. These errors requires further investigation to determine their cause.

Next, we estimated the partial contact position in real-time. Images of this demonstration are shown in Fig. 11 (see also the attached movie). The pictures on the left show the actual suction cup state, and the charts on the right show the estimated position (red circles). The far side of the cup is displayed at the top of the chart. Figure 11(a) shows the contact with a finger, and Fig. 11(b) shows contact with the lid of the plastic case. When the cup is in full contact, red fills in the chart (Fig. 11(c)). It can be seen that the estimated contact state matches the actual one.

V. CONCLUSION

A new capacitive proximity sensor for suction cups was developed. The two functions that can be achieved with one sensor module having three electrodes are push-in detection and partial contact detection. Since this sensor detects deformation of the cup, in principle, it can be applied to deformable cups such as the bellows type in addition to the flat type. We briefly tried a sensor-based control, which determines the picking and placing heights by detecting the push-in stroke (see the attached movie).

In the future, we will try to extend the sensor's applications to controlling the tilt of an object. The sensor has the potential to detect not only partial contact but also the posuture of suction cup when it is carrying an object.

REFERENCES

[1] M. Hashimoto, Y. Domae, and S. Kaneko, "Review: Current Status and Future Trends on Robot Vision Technology," *Journal of Robotics and Mechatronics*, Vol. 29, No. 2, pp. 275-286, 2017.

[2] L. Pérez, Í. Rodríguez, N. Rodríguez, R. Usamentiaga and D. García, "Robot Guidance Using Machine Vision Techniques in Industrial Environments: A Comparative Review," *Sensors MDPI*, Vol. 16, No. 335, pp. 1-26, 2016.

[3] Z. Kappassov, J. A. Corrales and V. Perdereau, "Tactile sensing in dexterous robot hands—Review," *Robotics and Autonomous Systems*, Vol. 74, pp. 195–220, 2015.

[4] E. Donlon, S. Dong, M. Liu, J. Li, E. Adelson, and A. Rodriguez, "Gelslim: A high-resolution, compact, robust, and calibrated tactile-sensing finger," in *Proceedings of IEEE/RSJ International Conference on Intelligent Robots and Systems (IROS)*, pp. 1927-1934, 2018.

[5] A. Cirillo, P. Cirillo, G.D. Maria, C. Natale, and S. Pirozzi, "Control of linear and rotational slippage based on six-axis force/tactile sensor," In *Proceedings of IEEE International Conference on Robotics and Automation (ICRA)*, pp. 1587–1594, 2017.

[6] K. Hsiao, P. Nangeroni, M. Huber, A. Saxena, and A. Y. Ng, "Reactive grasping using optical proximity sensors," in *Proceedings of IEEE International Conference on Robotics and Automation (ICRA)*, pp. 2098–2105, 2006.

[7] B. Yang, P. Lancaster, and J.R. Smith, "Pre-touch sensing for sequential manipulation," in *Proceedings of IEEE International Conference on Robotics and Automation (ICRA)*, pp. 5088-5095, 2017.

[8] K. Koyama, Y. Suzuki, A. Ming, and M. Shimojo, "Integrated Control of a Multi-fingered Hand and Arm using Proximity Sensors on the Fingertips," in *Proceedings of IEEE International Conference on Robotics and Automation (ICRA)*, pp. 4282-4288, 2016.

[9] K. Koyama, M. Shimojo, T. Senoo and M. Ishikawa, "High-Speed High-Precision Proximity Sensor for Detection of Tilt, Distance and Contact", *IEEE Robotics and Automation Letters*, Vol. 3, No. 4, pp. 3224–3231, 2018.

[10] N. Yamaguchi, S. Hasegawa, K. Okada and M. Inaba, "A Gripper for Object Search and Grasp through Proximity Sensing," in *Proceedings of IEEE/RSJ International Conference on Intelligent Robots and Systems (IROS)*, pp. 6690-6697, 2018.

[11] S. E. Navarro, M. Schonert, B. Hein, and H. Wörn, "6d proximity servoing for preshaping and haptic exploration using capacitive tactile proximity sensors," in *Proceedings of IEEE/RSJ International Conference on Intelligent Robots and Systems (IROS)*, pp. 7-14, 2014.

[12] R. Araki, F. Suga, T. Abe, H. Noma, and M. Sohgawa, "Gripping control of delicate and flexible object by electromotive manipulator with proximity and tactile combo MEMS sensor," *Transducers 2017*, pp. 1140-1143, 2017.

[13] A. Yamaguchi, "FingerVision for Tactile Behaviors, Manipulation, and Haptic Feedback Teleoperation, " in *Proceedings of the IEEJ International Workshop on Sensing, Actuation, Motion Control, and Optimization (SAMCON2018)*, IS2-4, 2018.

[14] R. Patel, R. Cox, and N. Correll, "Integrated proximity, contact and force sensing using elastomer-embedded commodity proximity sensors," *Autonomous Robots*, Vol. 42, No. 7, pp. 1443–1458, 2018.

[15] N. Correll, K. Bekris, D. Berenson, O. Brock, A. Causo, K. Hauser, K. Okada, A. Rodriguez, J. Romano, and P. Wurman, "Analysis and observations from the first Amazon Picking Challenge," *IEEE Trans. Automation Science and Engineering*, Vol. 15, No. 1, pp. 172–188, 2018.

[16] H. Nakamoto, M. Ohtake, K. Komoda, A. Sugahara and A. Ogawa , "A Gripper System for Robustly Picking Various Objects Placed Densely by Suction and Pinching," in *Proceedings of IEEE/RSJ International Conference on Intelligent Robots and Systems (IROS)*, pp. 6093-6098, 2018.

[17] C. Eppner, S. Höfer, R. Jonschkowski, R. Martín-Martín, A. Sieverling, V. Wall, and O. Brock, "Lessons from the Amazon Picking Challenge: Four aspects of building robotic systems," in *Proceedings of Robotics: Science and Systems*, 2016.

[18] K.T. Yu and A. Rodriguez, "Realtime state estimation with tactile and visual sensing for inserting a suction-held object," in *Proceedings of IEEE/RSJ International Conference on Intelligent Robots and Systems (IROS)*, pp. 1628–1635, 2018.

[19] V. Müller, T.-L. Lam and N. Elkmann, "Sensor Design and Model-based Tactile Feature Recognition," *2017 IEEE Sensors*, pp. 1-3, 2017.